BMC Cancer

RESEARCH Open Access

Preclinical evaluation of a fluorinated bifendate derivative in triple-negative breast cancer: integrated in vitro and in vivo evidence of antitumor activity

Lisa Zongyong Lin[1†], Hai-yi Huang[2,1†], Yuanyuan Peng[3], Guo-Qiang Lin[4], Jinbo Hu[3*] and Ying Jiang[1,2*]

Abstract

Background Triple-negative breast cancer (TNBC) is an aggressive subtype of breast cancer with limited therapeutic options and poor clinical outcomes. Bifendate (DDB), a clinically used hepatoprotective agent, has shown modest antitumor activity.

This study evaluated the antitumor activity of a fluorinated bifendate derivative (F-α-DDB-derivative) in TNBC models.

Methods MDA-MB-468 cells were treated with DDB or F-α-DDB-derivative to assess cell viability, migration, apoptosis, and Ki-67 expression. Antitumor efficacy and preliminary safety were further evaluated in a nude mouse xenograft model.

Results F-α-DDB-derivative reduced cell viability in a concentration-dependent manner and showed greater potency than DDB, with a 24 h IC_{50} of 25.06 μg/mL versus 105.00 μg/mL for DDB. At 25 μg/mL, F-α-DDB-derivative significantly inhibited migration compared with the control group, reduced Ki-67 expression, increased apoptosis, and showed stronger antitumor activity than DDB in most evaluated assays. In vivo, intraperitoneal administration of F-α-DDB-derivative (20 mg/kg, every other day for 14 days) significantly suppressed tumor growth and reduced final tumor weight compared with both the control and DDB groups. No significant abnormalities in body weight or serum biochemical markers were observed under the tested conditions.

Conclusions Fluorination enhanced the antitumor activity of DDB in TNBC models. F-α-DDB-derivative represents a promising fluorinated lead compound for further preclinical investigation.

Keywords Antitumor activity, Bifendate, F-α-DDB-derivative, Preclinical study, Triple-negative breast cancer, Xenograft

†Lisa Zongyong Lin and Hai-yi Huang contributed equally to this work.

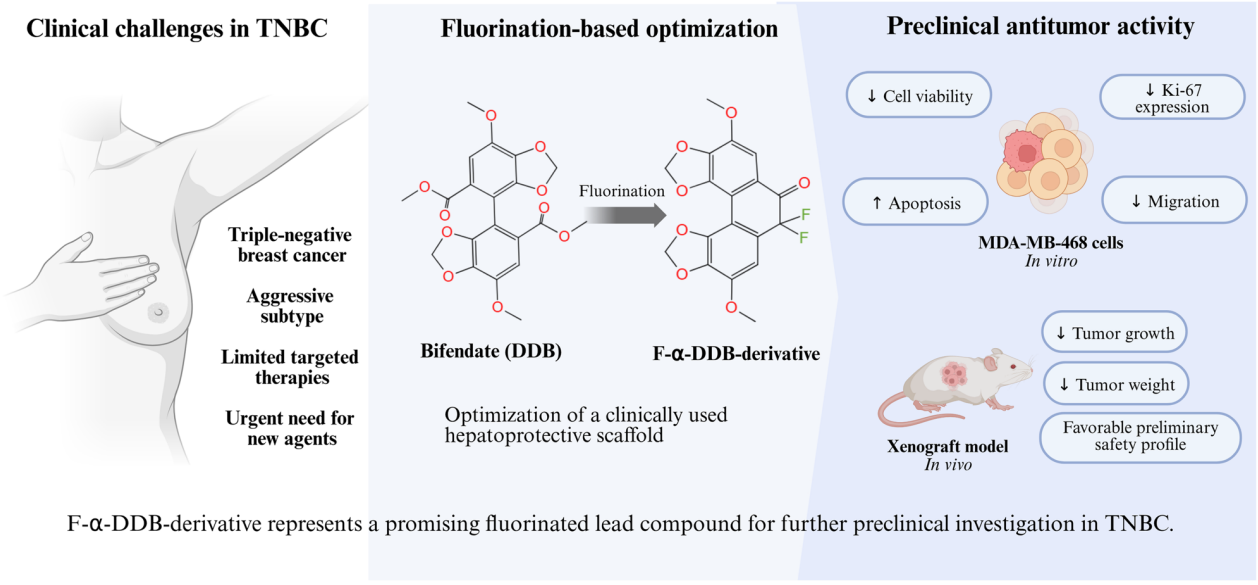
*Correspondence:
Ying Jiang
jiang.ying3@zs-hospital.sh.cn
Jinbo Hu
jinbohu@sioc.ac.cn

Full list of author information is available at the end of the article

© The Author(s) 2026. **Open Access** This article is licensed under a Creative Commons Attribution-NonCommercial-NoDerivatives 4.0 International License, which permits any non-commercial use, sharing, distribution and reproduction in any medium or format, as long as you give appropriate credit to the original author(s) and the source, provide a link to the Creative Commons licence, and indicate if you modified the licensed material. You do not have permission under this licence to share adapted material derived from this article or parts of it. The images or other third party material in this article are included in the article's Creative Commons licence, unless indicated otherwise in a credit line to the material. If material is not included in the article's Creative Commons licence and your intended use is not permitted by statutory regulation or exceeds the permitted use, you will need to obtain permission directly from the copyright holder. To view a copy of this licence, visit http://creativecommons.org/licenses/by-nc-nd/4.0/.

Graphical Abstract

F-α-DDB-derivative, generated by fluorination-based optimization of bifendate, showed enhanced antitumor activity in triple-negative breast cancer models by suppressing malignant phenotypes in vitro and inhibiting xenograft growth with a favorable preliminary safety profile.



Background

Breast cancer (BC) is the most commonly diagnosed malignancy in women worldwide and remains a leading cause of cancer-related death [1]. Based on gene expression profiling, BC can be classified into several molecular subtypes with distinct biological behaviors and clinical outcomes [2, 3]. Current treatment strategies for BC include surgery, radiotherapy, chemotherapy, endocrine therapy, HER2-targeted therapy, immunotherapy, antibody–drug conjugates, and other emerging targeted approaches [4–6]. Endocrine therapies, including aromatase inhibitors, are mainly used for hormone receptor-positive BC, whereas HER2-targeted agents are used for HER2-positive disease. Among the molecular subtypes, triple-negative breast cancer (TNBC), which lacks estrogen receptor (ER), progesterone receptor (PR), and human epidermal growth factor receptor 2 (HER2) expression, accounts for approximately 10–20% of all BC cases and is considered one of the most aggressive subtypes [7, 8]. Because of the absence of ER, PR, and HER2 expression, endocrine therapy and HER2-targeted therapy are generally not applicable to TNBC, which has encouraged the investigation of alternative small-molecule and molecularly targeted therapeutic strategies [9–11]. Although TNBC may initially respond to chemotherapy, it is associated with high rates of recurrence and metastasis and generally has a poor prognosis [12, 13]. Despite recent advances, chemotherapy remains an important component of systemic treatment for TNBC, and the clinical benefit of newer therapeutic strategies remains limited for many patients [4–6].

Therefore, the development of safe and effective novel therapeutic agents for TNBC remains an urgent clinical need.

Bifendate (DDB) (Fig. 1A), a synthetic intermediate of schisandrin C derived from *Schisandra chinensis*, is a clinically used hepatoprotective agent for chronic liver diseases with good tolerability [14]. Increasing evidence has suggested that DDB also possesses potential antitumor activity, particularly in inhibiting tumor cell invasion and regulating invasion-related molecules [15, 16]. However, our preliminary studies indicated that DDB exhibits only modest antitumor efficacy in breast cancer and requires relatively high concentrations to achieve measurable effects. These findings suggest that DDB may serve as a reasonable scaffold for structural optimization aimed at improving antitumor efficacy while retaining its favorable safety profile.

Fluorination is a widely used strategy in modern medicinal chemistry for optimizing drug properties, and approximately 25% of clinically approved small-molecule drugs contain fluorine atoms or fluorinated moieties [17, 18]. The introduction of fluorine can alter the electronic distribution, lipophilicity, molecular conformation, and metabolic stability of drug molecules, thereby improving

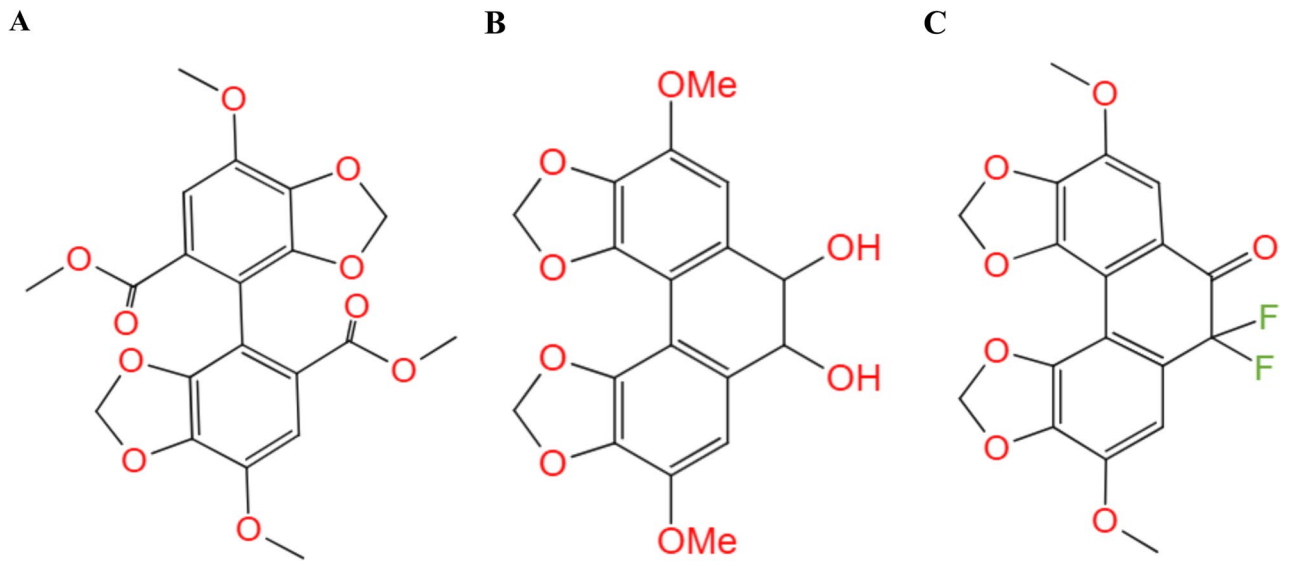


Fig. 1 Chemical structures of bifendate and its derivatives. **A** Chemical structure of bifendate (DDB); **B** chemical structure of Compound A, the precursor used for the synthesis of F-α-DDB-derivative; **C** complete chemical structure of F-α-DDB-derivative, chemically named 7,7-difluoro-4,9-dimethoxyphenanthro [3,4-d:5,6-d']bis ([1, 3] dioxole)-6(7 H)-one

biological activity and pharmacokinetic properties [17, 18]. In collaboration with the Shanghai Institute of Organic Chemistry, Chinese Academy of Sciences, we designed and synthesized an α-fluorinated bifendate derivative (F-α-DDB-derivative) (Fig. 1C) using Compound A (Fig. 1B) as the lead compound, with the aim of enhancing the antitumor potential of DDB. Our previous study showed that F-α-DDB-derivative combined with epirubicin improved antitumor efficacy against TNBC without causing additional cardiotoxicity [19]. However, the independent antitumor activity of F-α-DDB-derivative and its comparative efficacy relative to DDB have not been fully characterized.

In this study, we systematically evaluated the antitumor effects of F-α-DDB-derivative against TNBC using both in vitro and in vivo models. We assessed its effects on cell proliferation, migration, apoptosis, and Ki-67 expression, and further examined its antitumor efficacy and preliminary safety in a nude mouse xenograft model. To our knowledge, this study provides the first integrated in vitro and in vivo evaluation of F-α-DDB-derivative in TNBC and establishes a preliminary basis for its further preclinical development as a fluorinated antitumor lead compound.

Materials and methods

Cell lines and cell culture

The human triple-negative breast cancer cell line MDA-MB-468 was obtained from Procell (Wuhan, China). Cells were cultured in Dulbecco's Modified Eagle Medium (DMEM, CM-0290B; Procell, Wuhan, China) supplemented with 10% fetal bovine serum (FBS) and 1% penicillin/streptomycin (P/S), and maintained at 37 °C in a humidified incubator with 5% CO_2 (Thermo Scientific, USA). Cell culture and passaging were performed under standard aseptic conditions.

Experimental animals

Female BALB/c nude mice (4–6 weeks old, 18–21 g) were obtained from the Shanghai Model Organisms Center, Inc. (Shanghai, China). Animals were housed under specific pathogen-free (SPF) conditions at 23–26 °C and 40–60% humidity, with free access to sterilized food and filtered water. All animal procedures were conducted in accordance with the guidelines of the Institutional Animal Care and Use Committee of the Shanghai Model Organisms Center, Inc. (SRCMO-IACUC No. 2024-0003) and were approved prior to the initiation of the study. Tumor dimensions were monitored throughout the study using calipers, and no animals exceeded the approved tumor size limits.

Reagents

Bifendate (DDB, BD40653) was purchased from Bide Pharmatech (Shanghai, China).

F-α-DDB-derivative, chemically named 7,7-difluoro-4,9-dimethoxyphenanthro[3,4-d:5,6-d']bis([1, 3]dioxole)-6(7 H)-one, was synthesized and characterized by Yuanyuan Peng under the supervision of Jinbo Hu at the Shanghai Institute of Organic Chemistry, Chinese Academy of Sciences (Shanghai, China). Compound A, the precursor used for the synthesis of F-α-DDB-derivative, was derived from precursor-related chemical work established by Guo-Qiang Lin and colleagues. The

synthesis and structural characterization of F-α-DDB-derivative are provided in the Supplementary Information. Dimethyl sulfoxide (DMSO) was purchased from Sigma-Aldrich (Gillingham, UK). Trypsin (0.25%, KGL2102-100) was obtained from Beyotime Institute of Biotechnology (Haimen, China). PEG300 was purchased from MedChemExpress (New Jersey, USA), and Tween 80 was obtained from Aladdin (Shanghai, China).

Cell viability assay

Cell viability was evaluated using a Cell Counting Kit-8 (CCK-8) assay as previously described, with minor modifications [20, 21]. Briefly, MDA-MB-468 cells were seeded into 96-well plates at a density of 1 × 10^5 cells/well and allowed to adhere for 24 h. The cells were then treated with different concentrations of DDB or F-α-DDB-derivative for 24 h. Each condition was tested in triplicate wells. After treatment, CCK-8 reagent (C0039; Beyotime Biotechnology, Shanghai, China) was added according to the manufacturer's instructions, and absorbance was measured at 450 nm using a microplate reader (Thermo Scientific, USA). Cell viability was expressed as a percentage relative to the control group, and IC_{50} values were calculated using GraphPad Prism 9.0 software.

Wound healing assay

Cell migration was assessed using a wound healing assay as previously described, with minor modifications [20, 22]. MDA-MB-468 cells were seeded in 6-well plates and cultured until approximately 90% confluence. A straight scratch was made using a sterile pipette tip, and detached cells were removed by washing with PBS. The cells were then cultured in serum-free medium containing DDB (25 μg/mL) or F-α-DDB-derivative (25 μg/mL), with an untreated control group included. Images of the wounded area were captured at 0 and 24 h under an inverted microscope, and migration was quantified by measuring the wound closure area using ImageJ software.

Apoptosis assay

Cell apoptosis was assessed by flow cytometry using Annexin V-APC/DAPI double staining according to previously reported methods, with minor modifications [20, 21].

MDA-MB-468 cells were seeded in 6-well plates and cultured for 24 h, followed by treatment with DDB (25 μg/mL) or F-α-DDB-derivative (25 μg/mL), with an untreated control group included. After 24 h of treatment, the cells were harvested and stained with an Annexin V Apoptosis Detection Kit APC (88-8007-72; Thermo Fisher Scientific, USA) according to the manufacturer's instructions. Apoptotic cells were analyzed using a flow cytometer (Beckman Coulter, USA), and the total apoptosis rate was calculated as the sum of early and late apoptotic cells.

Immunofluorescence assay for Ki-67

Ki-67 immunofluorescence staining was performed to evaluate proliferative activity using a commercial Ki-67 Cell Proliferation Assay Kit according to the manufacturer's instructions, with minor modifications. Ki-67 was used as a proliferation marker based on its established relevance in breast cancer [23–25].

MDA-MB-468 cells were seeded in 6-well plates and cultured for 24 h, followed by treatment with DDB (25 μg/mL) or F-α-DDB-derivative (25 μg/mL) for 24 h, with an untreated control group included. After treatment, the cells were washed with PBS, fixed, and blocked with immunostaining blocking buffer. The cells were then incubated overnight at 4 °C with anti-Ki-67 mouse monoclonal antibody using a Ki-67 Cell Proliferation Assay Kit (IF, Red, Mouse mAb; C2312S, Beyotime Biotechnology, Shanghai, China), followed by incubation with Cy3-conjugated anti-mouse secondary antibody and DAPI staining. Fluorescence images were captured under a fluorescence microscope, and Ki-67 expression was quantified by measuring the percentage of Ki-67-positive area using ImageJ software.

In vivo xenograft experiment

The MDA-MB-468 xenograft model was established as previously described, with minor modifications [20]. MDA-MB-468 cells (1×10^6) were resuspended in a 1:1 mixture of DMEM and Matrigel (Corning, NY, USA), and a total volume of 200 μL was subcutaneously injected into the fourth mammary fat pad on the right side of each mouse. Eighteen mice were initially randomized into three groups (n = 6 per group): control, DDB, and F-α-DDB-derivative. Tumor length (L) and width (W) were measured using calipers, and tumor volume was calculated as $V = L \times W^2 / 2$. Treatment was initiated when the mean tumor volume reached approximately 103 mm^3.

DDB and F-α-DDB-derivative were formulated in a vehicle consisting of 5% DMSO, 40% PEG300, 5% Tween-80, and 50% normal saline. Mice in the treatment groups received DDB (20 mg/kg) or F-α-DDB-derivative (20 mg/kg) by intraperitoneal injection every other day for 14 days, while mice in the control group received an equal volume of the vehicle. Body weight and tumor volume were recorded every 2 days during treatment. During the experiment, two mice died due to fighting-related injuries. Therefore, the final number of animals included in the endpoint analysis was $n = 5$ per group.

At the end of the experiment, mice were anesthetized with isoflurane in oxygen, and terminal blood samples were collected under deep anesthesia. After confirmation of loss of consciousness, the animals were euthanized by

cervical dislocation. Death was confirmed by the absence of corneal reflex and cessation of breathing for more than 1 min. This method was selected to minimize pain and distress and to allow terminal blood collection and tissue harvest in accordance with institutional guidelines. Tumors were then excised and weighed immediately after dissection. Serum levels of ALT, AST, UREA, CREA, CK, CK-MB, and LDH were measured using the corresponding assay kits (Rayto, Shenzhen, China) and an automated biochemical analyzer. Tumor tissues were then fixed in paraformaldehyde, embedded in paraffin, and subjected to hematoxylin and eosin (H&E) staining for histological examination.

Statistical analysis

All in vitro experiments were performed independently at least three times, and data are presented as the mean ± standard deviation (SD). For the in vivo study, the final number of animals included in the endpoint analysis was $n = 5$ per group. Statistical analyses were performed using one-way analysis of variance (ANOVA) followed by Dunnett's post hoc test in GraphPad Prism 9.0 (GraphPad Software, San Diego, CA, USA). A value of $P < 0.05$ was considered statistically significant.

Results

Effects of F-α-DDB-derivative on the viability of MDA-MB-468 cells

Compared with the control group, both DDB and F-α-DDB-derivative reduced the viability of MDA-MB-468 cells in a concentration-dependent manner (Fig. 2A, B). At comparable concentrations, F-α-DDB-derivative showed a stronger inhibitory effect than DDB (Fig. 2C). The 24 h IC_{50} values of DDB and F-α-DDB-derivative were 105.00 and 25.06 μg/mL, respectively, indicating that F-α-DDB-derivative was more potent than DDB. Based on these results, 25 μg/mL was selected for subsequent experiments.

F-α-DDB-derivative inhibits the migration of MDA-MB-468 cells

Wound healing analysis showed that the migration rates of MDA-MB-468 cells in the control, DDB, and F-α-DDB-derivative groups were 16.92 ± 5.41%, 13.04 ± 0.90%, and 6.09 ± 1.11%, respectively. Compared with the control group, F-α-DDB-derivative (25 μg/mL) significantly inhibited cell migration. DDB treatment also showed a slight reduction in migration, but the difference did not reach statistical significance. The migration rate in the F-α-DDB-derivative group was lower than that in the DDB group, but the difference did not reach statistical significance (Fig. 3).

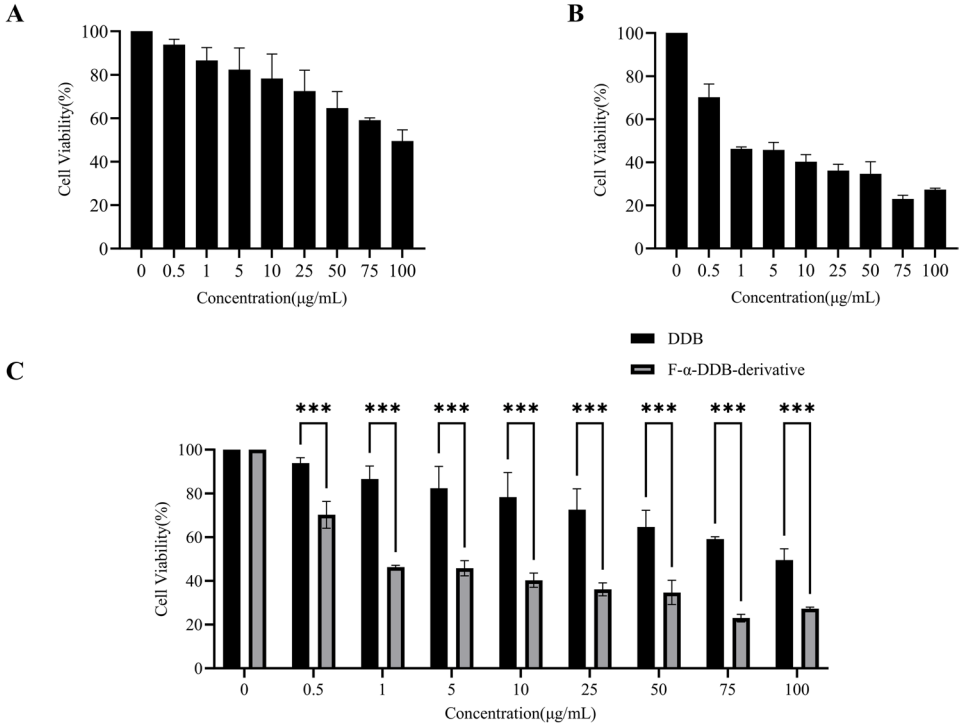


Fig. 2 F-α-DDB-derivative inhibits the viability of MDA-MB-468 cells in a concentration-dependent manner. **A** Viability of MDA-MB-468 cells treated with increasing concentrations of DDB. **B** Viability of MDA-MB-468 cells treated with increasing concentrations of F-α-DDB-derivative. **C** Comparison of the inhibitory effects of DDB and F-α-DDB-derivative on MDA-MB-468 cell viability. Data are presented as mean ± SD ($n = 3$). ***$P < 0.001$; ns, not significant

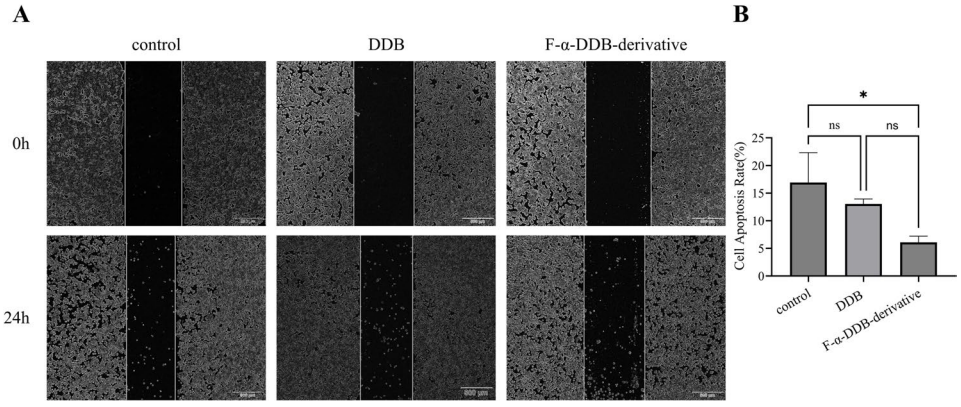


Fig. 3 F-α-DDB-derivative suppresses the migration of MDA-MB-468 cells. **A** Representative inverted microscope images from the wound healing assay at 0 and 24 h after treatment with DDB (25 μg/mL) or F-α-DDB-derivative (25 μg/mL) (4× objective). **B** Quantification of migration rates in each group. Data are presented as mean ± SD ($n = 3$). *$P < 0.05$; ns, not significant

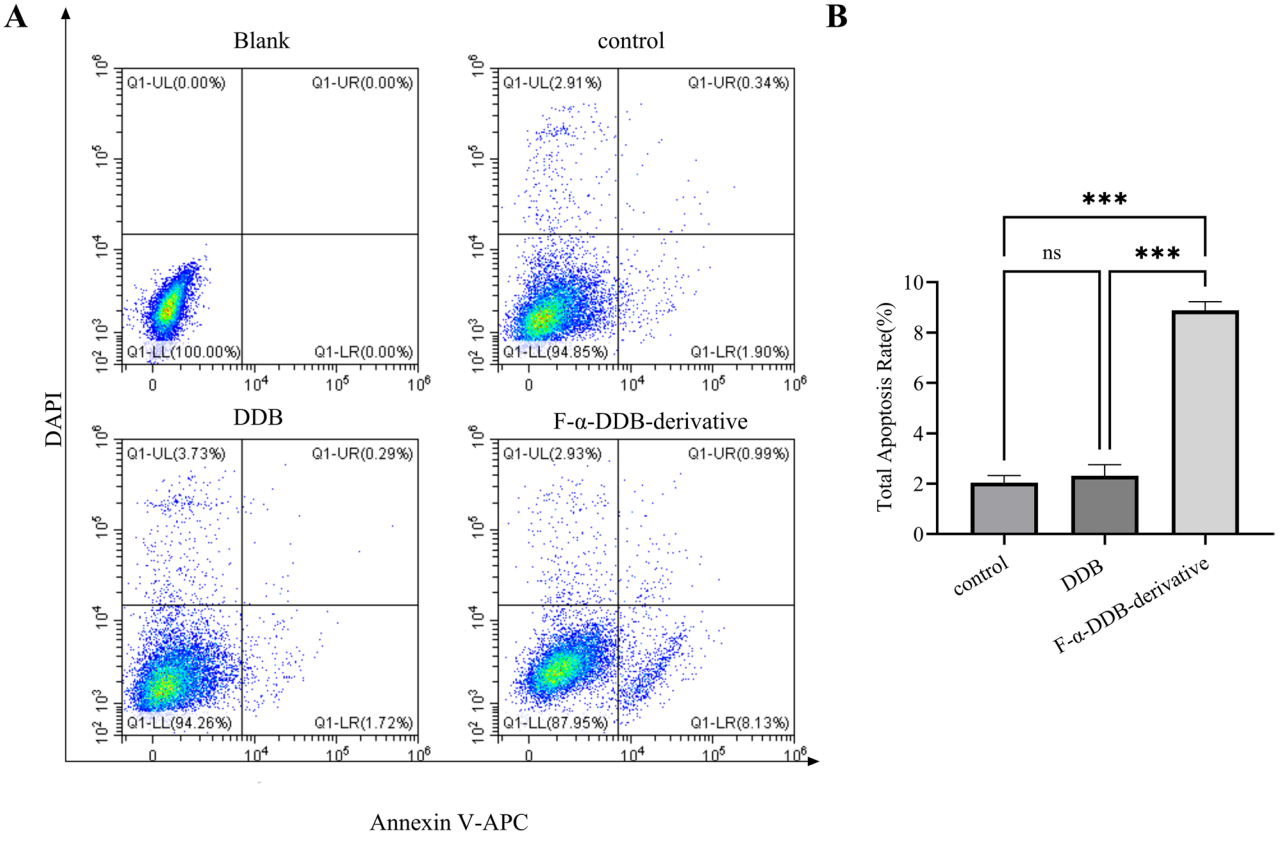


Fig. 4 F-α-DDB-derivative induces apoptosis in MDA-MB-468 cells. **A** Representative flow cytometry plots of Annexin V-APC/DAPI double staining in MDA-MB-468 cells after 24 h of treatment with DDB (25 μg/mL) or F-α-DDB-derivative (25 μg/mL). **B** Quantification of the total apoptosis rate (early + late apoptosis) in each group. Data are presented as mean ± SD ($n = 3$). ***$P < 0.001$; ns, not significant

Effects of F-α-DDB-derivative on apoptosis in MDA-MB-468 cells

Cell apoptosis was evaluated by flow cytometry using Annexin V-APC/DAPI double staining. Compared with the control group, F-α-DDB-derivative significantly increased the total apoptosis rate in MDA-MB-468 cells after 24 h of treatment. In contrast, DDB at the same concentration showed no significant effect on apoptosis. In addition, the total apoptosis rate in the F-α-DDB-derivative group was significantly higher than that in the DDB group, indicating that F-α-DDB-derivative exerted a stronger pro-apoptotic effect than the parent compound DDB (Fig. 4).

F-α-DDB-derivative reduces Ki-67 expression in MDA-MB-468 cells

Ki-67 immunofluorescence staining was performed to assess the effect of F-α-DDB-derivative on cell proliferative activity. Compared with the control group, treatment with F-α-DDB-derivative significantly reduced the percentage of Ki-67-positive area in MDA-MB-468 cells after 24 h, indicating decreased proliferative activity. DDB also reduced the percentage of Ki-67-positive area, but the difference did not reach statistical significance. Furthermore, the percentage of Ki-67-positive area in the F-α-DDB-derivative group was significantly lower than that in the DDB group. These findings suggest that F-α-DDB-derivative exerts a stronger inhibitory effect on the proliferation of MDA-MB-468 cells than the parent compound DDB (Fig. 5).

In vivo antitumor effects of F-α-DDB-derivative

Eighteen mice were initially assigned to three groups ($n = 6$ per group). During the experiment, two mice were lost due to fighting-related injuries; therefore, the final number of animals included in the endpoint analysis was $n = 5$ per group.

No significant differences in body weight were observed among the three groups during the treatment period (Fig. 6A). In addition, no obvious abnormalities in daily activity or food intake were noted, suggesting acceptable tolerability under the tested conditions.

From day 9 after treatment initiation, tumor volumes in the F-α-DDB-derivative group were significantly lower than those in both the control and DDB groups (Fig. 6B). Consistently, the final tumor weights, measured immediately after tumor dissection at the end of the experiment, were also significantly lower in the F-α-DDB-derivative group than in the control and DDB groups (Fig. 6C).

Histological analysis by H&E staining revealed marked morphological changes in the F-α-DDB-derivative group, including increased necrosis and fibrosis, together with fewer mitotic figures than in the control and DDB groups (Fig. 6D).

Effects of F-α-DDB-derivative on cardiac, hepatic, and renal function in vivo

To preliminarily evaluate systemic toxicity in vivo, serum biochemical markers related to hepatic, renal, and cardiac function were measured at the end of the experiment. No significant differences were observed among the three groups in serum ALT, AST, UREA, CREA, CK, CK-MB, or LDH levels. These results suggest that F-α-DDB-derivative did not cause significant alterations in the measured biochemical markers under the tested conditions (Fig. 7).

Discussion

TNBC is a highly aggressive breast cancer subtype with limited treatment options and poor clinical outcomes. Although chemotherapy remains the cornerstone of systemic treatment, its clinical utility is often constrained by toxicity and the high likelihood of recurrence and metastasis. Therefore, the development of novel agents with improved antitumor efficacy and acceptable tolerability

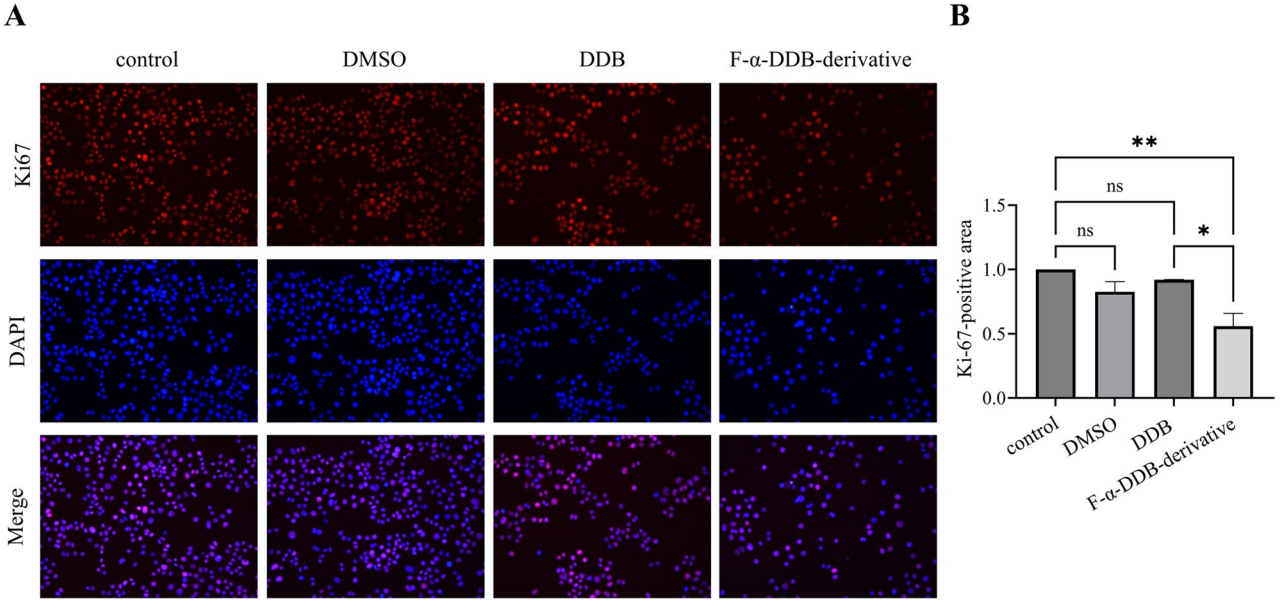


Fig. 5 F-α-DDB-derivative reduces Ki-67 expression in MDA-MB-468 cells. **A** Representative immunofluorescence images of Ki-67 staining after 24 h of treatment (10× objective; scale bar = 10 μm). **B** Quantification of the percentage of Ki-67-positive area in each group. Data are presented as mean ± SD ($n = 3$). *$P < 0.05$, **$P < 0.01$; ns, not significant

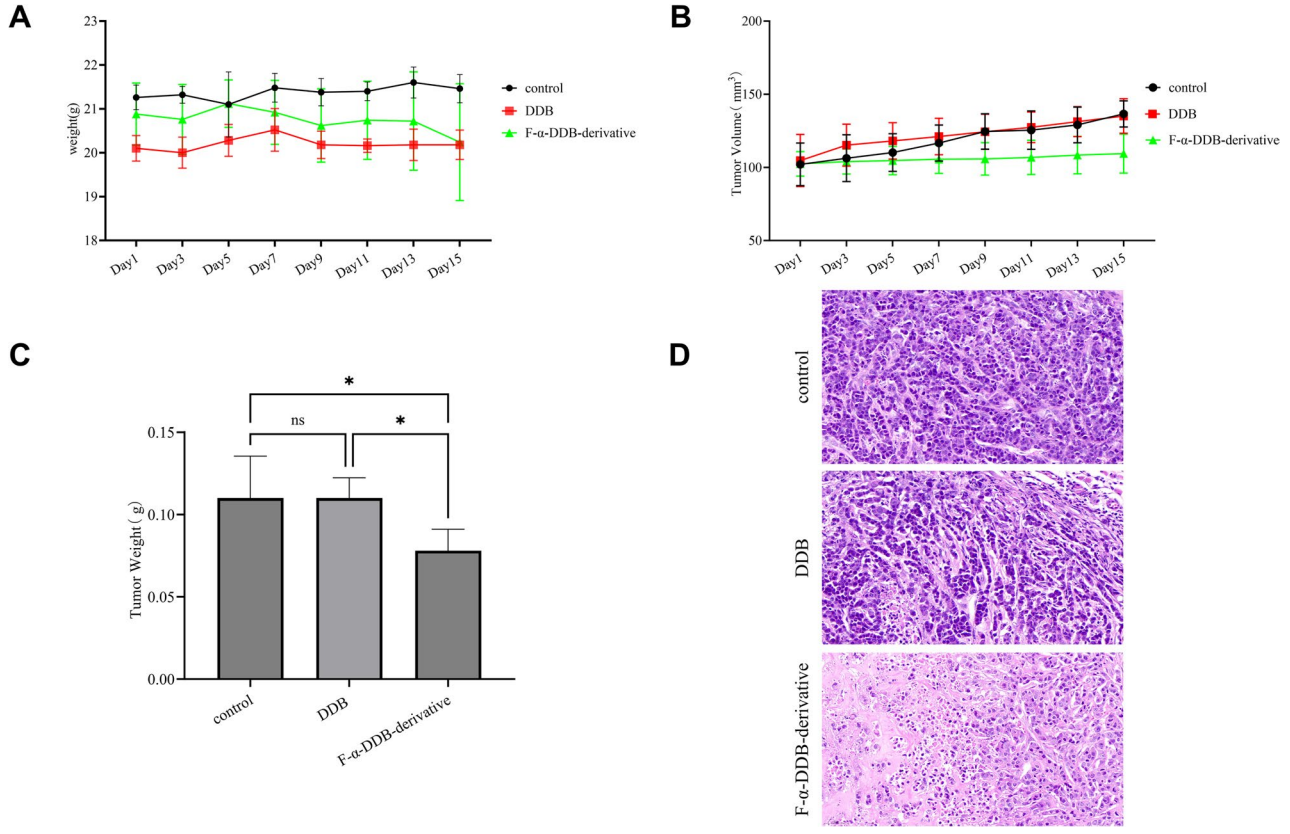


Fig. 6 In vivo antitumor effects of F-α-DDB-derivative in an MDA-MB-468 xenograft model. **A** Body weight changes in nude mice of each group during the 14-day treatment period. **B** Tumor growth curves of each group after treatment initiation. **C** Final tumor weights in each group. **D** Representative H&E-stained images of tumor tissues (scale bar = 100 μm). Data are presented as mean ± SD ($n = 5$). *$P < 0.05$; ns, not significant

remains an important goal in TNBC research [6–8, 26, 27].

DDB is a clinically used hepatoprotective agent with a favorable safety background and has also been reported to possess certain antitumor properties, particularly in relation to tumor invasion and invasion-associated molecules [14–16]. However, its relatively modest activity in breast cancer suggests that DDB itself may be more valuable as a scaffold for optimization than as a direct anticancer candidate. From this perspective, fluorination represents a rational modification strategy. In medicinal chemistry, fluorination is widely used to improve the biological performance of small molecules by influencing lipophilicity, molecular conformation, metabolic stability, and target interaction [17, 18]. Taken together, the stronger activity observed for F-α-DDB-derivative in the present study suggests that fluorination may enhance the antitumor potential of the DDB scaffold and provides preliminary pharmacological support for this optimization strategy.

The antitumor activity of F-α-DDB-derivative is supported not by a single experimental endpoint, but by a convergent pattern across several complementary assays. Reduced cell viability and decreased Ki-67 expression suggest suppression of proliferative capacity, whereas increased apoptosis indicates that activation of cell death also contributes to the overall inhibitory effect. In addition, the wound healing assay suggested reduced migratory behavior after treatment. Because wound closure may be influenced by both migration and proliferation, this result should not be interpreted in isolation [28, 29]. Instead, its value lies in its consistency with the CCK-8 and Ki-67 findings, which together support an overall inhibitory effect on malignant cell behavior. Similarly, the reduction in Ki-67 and the increase in apoptosis are biologically meaningful, because Ki-67 is a well-established marker of tumor proliferation in breast cancer, including TNBC, whereas induction of apoptotic cell death is a therapeutically relevant mechanism in anticancer treatment [23–25, 30, 31].

The in vivo findings further strengthen the significance of the in vitro observations. In a xenograft model, the ability of F-α-DDB-derivative to suppress tumor growth indicates that its activity is not restricted to simplified in vitro conditions but can also be reproduced in a living system. This is particularly important in early-stage preclinical evaluation, because in vivo efficacy provides stronger support for therapeutic potential than cell-based

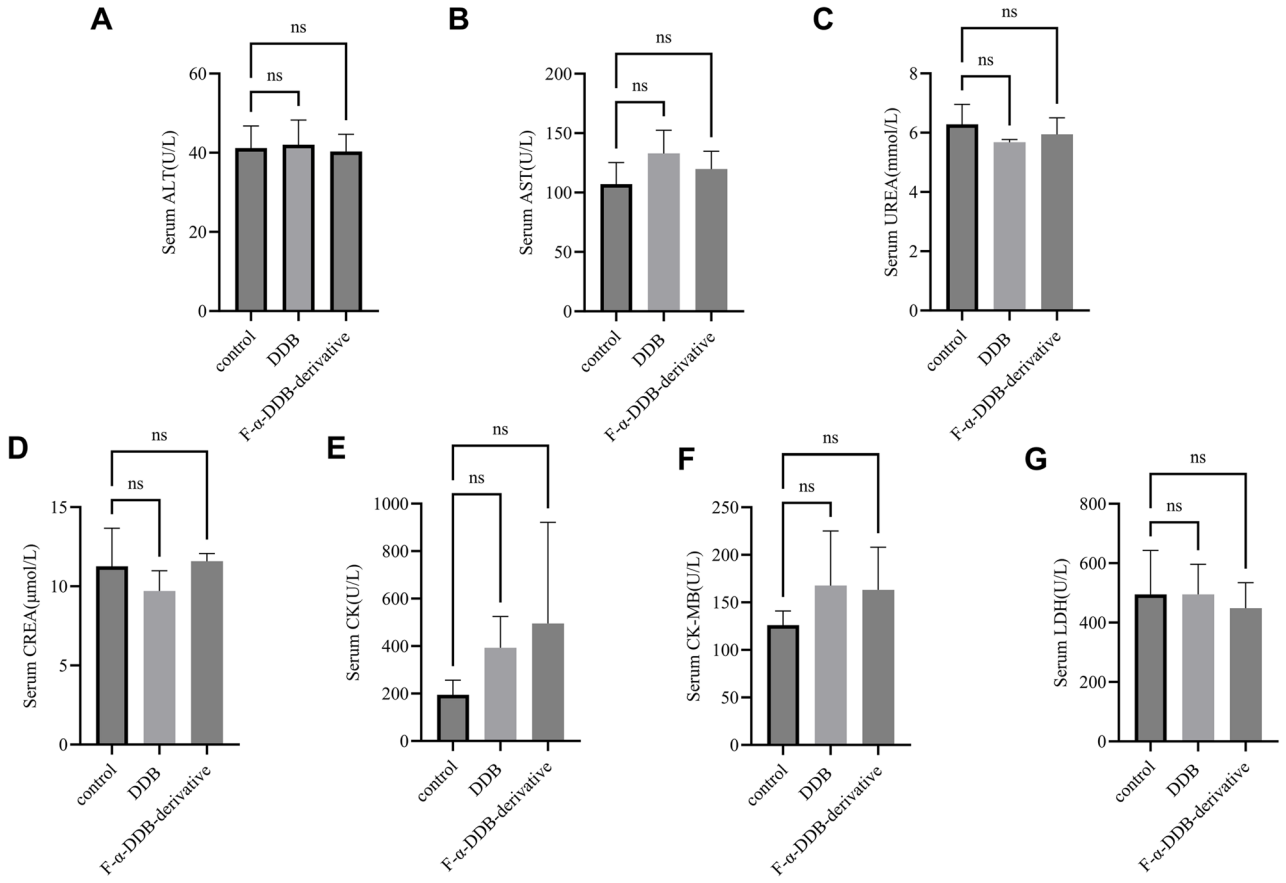


Fig. 7 Effects of F-α-DDB-derivative on serum biochemical markers related to hepatic, renal, and cardiac function under the tested conditions. Serum levels of biomarkers related to hepatic, renal, and cardiac function in each group: (**A**) ALT; (**B**) AST; (**C**) UREA; (**D**) CREA; (**E**) CK; (**F**) CK-MB; and (**G**) LDH. Data are presented as mean ± SD ($n = 5$). ns, not significant

findings alone. At the same time, the absence of significant abnormalities in body weight and the measured biochemical markers suggests that the compound did not produce overt systemic toxicity under the tested conditions. Although this does not establish a full toxicological profile, it does support the feasibility of further preclinical investigation.

From a translational perspective, the present findings are meaningful because they suggest that a clinically used and relatively well-tolerated scaffold can be rationally modified to generate a derivative with improved antitumor activity. This approach may be especially relevant in TNBC, where the need for new therapeutic options remains substantial. Importantly, F-α-DDB-derivative generally outperformed the parent compound DDB across several major endpoints, supporting the view that the fluorinated compound may represent an optimized lead rather than simply another structural analogue.

Several signaling pathways may contribute to the effects observed in this study. In TNBC, the PI3K/Akt and MAPK/ERK pathways are closely associated with cell proliferation, survival, and migration [32–34]. The phenotypic changes induced by F-α-DDB-derivative make these pathways biologically plausible candidates for subsequent mechanistic investigation. However, the present study was designed primarily as a preclinical efficacy evaluation rather than a mechanistic study. This is an important limitation, as the molecular basis of the enhanced activity remains undefined.

Nevertheless, this limitation is partially mitigated by the consistency of the findings across multiple in vitro assays, xenograft growth inhibition, and histological observations. Several additional methodological limitations should also be acknowledged. Only one TNBC cell line was used, which limits generalizability across the heterogeneous spectrum of TNBC. Migration was assessed using a wound healing assay, which is influenced by proliferation status as well as motility, although we partially addressed this by interpreting the migration results together with CCK-8 and Ki-67 data. In addition, two mice were lost because of fighting-related injuries, which reduced the final sample size for endpoint analysis. Despite this, the overall antitumor trend remained consistent across tumor volume, tumor weight, and histological assessment. Future studies should therefore focus on mechanistic validation, broader evaluation across

additional TNBC models, and characterization of pharmacokinetics, long-term safety, and potential combination strategies.

Conclusion

In conclusion, the present study provides preliminary evidence that fluorination-based optimization can enhance the antitumor potential of the DDB scaffold in TNBC.

F-α-DDB-derivative showed stronger overall antitumor activity than the parent compound DDB in both in vitro and in vivo models and demonstrated a favorable preliminary safety profile under the tested conditions. Although the molecular basis of its enhanced activity remains to be clarified, the consistency of the observed phenotypic effects supports its value as a promising fluorinated lead compound for further preclinical investigation in TNBC.

Abbreviations

ALT	Alanine aminotransferase
AST	Aspartate aminotransferase
BC	Breast cancer
CCK-8	Cell Counting Kit-8
CK	Creatine kinase
CK-MB	Creatine kinase-MB
CREA	Creatinine
DDB	Bifendate
DMEM	Dulbecco's Modified Eagle Medium
DMSO	Dimethyl sulfoxide
ER	Estrogen receptor
FBS	Fetal bovine serum
HER2	Human epidermal growth factor receptor 2
LDH	Lactate dehydrogenase
P/S	Penicillin/streptomycin
PBS	Phosphate-buffered saline
PR	Progesterone receptor
TNBC	Triple-negative breast cancer
UREA	Blood urea

Supplementary Information

The online version contains supplementary material available at https://doi.org/10.1186/s12885-026-16335-1.

Supplementary Material 1.

Acknowledgements

Not applicable.

Authors' contributions

YJ designed the biological study and supervised the overall project. LZYL and HYH performed the biological experiments. YP synthesized and characterized F-α-DDB-derivative. GQL contributed to the precursor-related chemical basis and precursor source of compound A. JH supervised the chemical synthesis and fluorination strategy. YJ, LZYL, HYH, YP, GQL, and JH analyzed and interpreted the data. LZYL and HYH drafted the manuscript. YJ and JH revised the manuscript. All authors read and approved the final manuscript.

Funding

This work was supported by Fujian Provincial Natural Science Foundation of China (2022J011416).

Data availability

The data supporting the findings of this study are available from the corresponding author upon reasonable request.

Declarations

Ethics approval and consent to participate

All animal procedures were approved by the Shanghai Model Organisms Center Institutional Animal Care and Use Committee (SRCMO-IACUC No. 2024-0003) and were performed in accordance with institutional guidelines and regulations. Tumor dimensions were monitored throughout the study using calipers, and no animals exceeded the approved tumor size limits. At the experimental endpoint, mice were anesthetized with isoflurane in oxygen and euthanized by cervical dislocation after confirmation of deep anesthesia and loss of consciousness. Death was confirmed by the absence of corneal reflex and cessation of breathing for more than 1 min.

Consent for publication

Not applicable.

Competing interests

The authors declare no competing interests.

Author details

[1]Department of General Surgery, Zhongshan Hospital, Fudan University, Shanghai, China
[2]Present address: Department of General Surgery, Xiamen Branch, Zhongshan Hospital, Fudan University, Fujian, China
[3]State Key Laboratory of Fluorine and Nitrogen Chemistry and Advanced Materials, Shanghai Institute of Organic Chemistry, University of Chinese Academy of Sciences, Chinese Academy of Sciences, 345 Lingling Road, Shanghai 200032, China
[4]State Key Laboratory of Chemical Biology, Shanghai Institute of Organic Chemistry, University of Chinese Academy of Sciences, Chinese Academy of Sciences, 345 Lingling Road, Shanghai 200032, China

Received: 10 April 2026 / Accepted: 8 June 2026
Published online: 12 June 2026

References

1. Siegel RL, Miller KD, Wagle NS, Jemal A. Cancer statistics, 2023. CA Cancer J Clin. 2023;73(1):17–48.
2. Sørlie T, Perou CM, Tibshirani R, Aas T, Geisler S, Johnsen H, Hastie T, Eisen MB, Van De Rijn M, Jeffrey SS. Gene expression patterns of breast carcinomas distinguish tumor subclasses with clinical implications. Proc Natl Acad Sci U S A. 2001;98(19):10869–74.
3. Sørlie T, Tibshirani R, Parker J, Hastie T, Marron JS, Nobel A, Deng S, Johnsen H, Pesich R, Geisler S. Repeated observation of breast tumor subtypes in independent gene expression data sets. Proc Natl Acad Sci U S A. 2003;100(14):8418–23.
4. Waks AG, Winer EP. Breast cancer treatment: a review. JAMA. 2019;321(3):288–300.
5. Tray N, Adams S, Esteva FJ. Antibody–drug conjugates in triple negative breast cancer. Future Oncol. 2018;14(25):2651–61.
6. Kalimutho M, Parsons K, Mittal D, López JA, Srihari S, Khanna KK. Targeted therapies for triple-negative breast cancer: combating a stubborn disease. Trends Pharmacol Sci. 2015;36(12):822–46.
7. Nishimura R, Osako T, Okumura Y, Nakano M, Otsuka H, Fujisue M, Arima N. Triple negative breast cancer: an analysis of the subtypes and the effects of menopausal status on invasive breast cancer. J Clin Med. 2022;11(9):2331.
8. Bianchini G, Balko JM, Mayer IA, Sanders ME, Gianni L. Triple-negative breast cancer: challenges and opportunities of a heterogeneous disease. Nat Rev Clin Oncol. 2016;13(11):674–90.
9. Ewieda SY, Ahmed EM, Gohar NA, Ibrahim SG, Essa MA, Nemr MTM. Design, synthesis, and antitumor evaluation of new pyridazinone scaffolds as dual EGFR/VEGFR-2 kinase inhibitors and apoptotic cells inducers. Bioorg Chem. 2025;166:109157.
10. Ewieda SY, Ahmed EM, Halim PA, Ibrahim SG, Gouda KM, Abdalla M, Eltayb WA, Nemr MTM. Discovery of novel pyridazinone derivatives as EGFRWT/EGFRT790M kinase inhibitors; design, synthesis, antitumor evaluation, and molecular dynamic simulations. Bioorg Chem. 2026;170:109486.
11. Fadaly WAA, Zidan TH, Kahk NM, Mohamed FEA, Abdelhakeem MM, Khalil RG, Nemr MTM. New pyrazolyl-thiazolidinone/thiazole derivatives as celecoxib/dasatinib analogues with selective COX-2, HER-2 and EGFR inhibitory effects:

design, synthesis, anti-inflammatory/anti-proliferative activities, apoptosis, molecular modelling and ADME studies. J Enzyme Inhib Med Chem. 2023;38(1):2281262.
12. Carey LA, Dees EC, Sawyer L, Gatti L, Moore DT, Collichio F, Ollila DW, Sartor CI, Graham ML, Perou CM. The triple negative paradox: primary tumor chemosensitivity of breast cancer subtypes. Clin Cancer Res. 2007;13(8):2329–34.
13. Nguyen PL, Taghian AG, Katz MS, Niemierko A, Abi Raad RF, Boon WL, Bellon JR, Wong JS, Smith BL, Harris JR. Breast cancer subtype approximated by estrogen receptor, progesterone receptor, and HER-2 is associated with local and distant recurrence after breast-conserving therapy. J Clin Oncol. 2008;26(14):2373–8.
14. Wang C, Xu YQ. Diphenyl dimethyl bicarboxylate in the treatment of viral hepatitis, adjuvant or curative? Gastroenterol Res. 2008;1(1):2.
15. Sun H, Liu G. The study of anti-hepatitis drug dimethyl dicarboxylate biphenyl on invasion of human hepatocellular carcinoma MHCC97-H cells and its active mechanisms. Chin Ger J Clin Oncol. 2008;7(1):2–6.
16. Sun H, Liu G-T. Inhibitory effect of dimethyl dicarboxylate biphenyl on invasion of human hepatocellular carcinoma cell line MHCC97-H with high metastasis potential and its mechanisms. Chin J Cancer. 2006;25(12):1464–9.
17. Kirk KL. Fluorine in medicinal chemistry: Recent therapeutic applications of fluorinated small molecules. J Fluor Chem. 2006;127(8):1013–29.
18. Gillis EP, Eastman KJ, Hill MD, Donnelly DJ, Meanwell NA. Applications of fluorine in medicinal chemistry. J Med Chem. 2015;58(21):8315–59.
19. Huang H-y, Lin LZY, Lu X-y, Jiang Y. F-α-DDB-derivative, a novel synthetic of bifendate, plus epirubicin improves antitumor efficacy against triple negative breast cancer without additional cardiotoxicity. Discover Oncol. 2025;16(1):690.
20. Zhou D-D, Bai W-Q, Zhai X-T, Sun L-P, Zhen Y-S, Li Z-R, Miao Q-F. Excellent effects and possible mechanisms of action of a new antibody–drug conjugate against EGFR-positive triple-negative breast cancer. Military Med Res. 2021;8(1):63.
21. Gao S, Zhang X, Liu J, Ji F, Zhang Z, Meng Q, Zhang Q, Han X, Wu H, Yin Y, Lv Y, Shi W. Icariin induces triple-negative breast cancer cell apoptosis and suppresses invasion by inhibiting the JNK/c-Jun signaling pathway. Drug Des Devel Ther. 2023;17(null):821–36.
22. Wang H, Zhao L, Wu J, Hong J, Wang S. Propofol induces ROS–mediated intrinsic apoptosis and migration in triple–negative breast cancer cells. Oncol Lett. 2020;20(1):810–6.
23. Davey MG, Hynes SO, Kerin MJ, Miller N, Lowery AJ. Ki-67 as a prognostic biomarker in invasive breast cancer. Cancers (Basel). 2021;13(17):4455.
24. Nielsen TO, Leung SCY, Rimm DL, Dodson A, Acs B, Badve S, Denkert C, Ellis MJ, Fineberg S, Flowers M. Assessment of Ki67 in breast cancer: updated recommendations from the international Ki67 in breast cancer working group. J Natl Cancer Inst. 2021;113(7):808–19.
25. Arafah MA, Ouban A, Ameer OZ, Quek KJ. KI-67 LI expression in triple-negative breast cancer patients and its significance. Breast Cancer (Auckl). 2021;15:11782234211016977.
26. Langeh U, Kumar V, Ahuja P, Singh C, Singh A. An update on breast cancer chemotherapy-associated toxicity and their management approaches. Health Sci Rev. 2023;9:100119.
27. Brown T, Sykes D, Allen AR. Implications of breast cancer chemotherapy-induced inflammation on the gut, liver, and central nervous system. Biomedicines. 2021;9(2):189.
28. Freitas JT, Jozic I, Bedogni B. Wound healing assay for melanoma cell migration. Melanoma: Methods and Protocols: Springer; 2021. p. 65–71.
29. Wang X, Decker CC, Zechner L, Krstin S, Wink M. In vitro wound healing of tumor cells: inhibition of cell migration by selected cytotoxic alkaloids. BMC Pharmacol Toxicol. 2019;20(1):4.
30. Labi V, Erlacher M. How cell death shapes cancer. Cell Death Dis. 2015;6(3):e1675–e.
31. Plati J, Bucur O, Khosravi-Far R. Apoptotic cell signaling in cancer progression and therapy. Integr Biol (Camb). 2011;3(4):279–96.
32. Bartholomeusz C, Gonzalez-Angulo AM, Liu P, Hayashi N, Lluch A, Ferrer-Lozano J, Hortobágyi GN. High ERK protein expression levels correlate with shorter survival in triple-negative breast cancer patients. Oncologist. 2012;17(6):766–74.
33. Hassan A, Aubel C. The PI3K/Akt/mTOR signaling pathway in triple-negative breast cancer: a resistance pathway and a prime target for targeted therapies. Cancers (Basel). 2025;17(13):2232.
34. Zhang H-p, Jiang R-y, Zhu J-y, Sun K-n, Huang Y, Zhou H-h, Zheng Y-b. Wang X-j. PI3K/AKT/mTOR signaling pathway: an important driver and therapeutic target in triple-negative breast cancer. Breast Cancer. 2024;31(4):539–51.

Publisher's note

Springer Nature remains neutral with regard to jurisdictional claims in published maps and institutional affiliations.